Post-print of Claramunt, S. et al. «Non-homogeneuos conduction of conductive filaments in Ni/HfO2/Si resistive switching structures observed with CAFM» in *Microelectronic engineering*, Vol. 147, (November 2015), p. 335-338. The final version is available at DOI 10.1016/j.mee.2015.04.112

Non-homogeneous conduction of conductive filaments in $Ni/HfO_2/Si$ resistive switching structures observed with CAFM

S. Claramunt[a,*], Q. Wu[a], M. Maestro[a], M. Porti[a], M. B. Gonzalez[b], J. Martin-Martinez[a], F. Campabadal[b], M. Nafría[a]

[a]*Universitat Autonoma de Barcelona. Dept. Enginyeria Electronica Edifici Q. 08193 Bellaterra, Spain*
[b]*Institut de Microelectronica de Barcelona, IMB-CNM (CSIC), Campus UAB,08193 Bellaterra, Spain*
[*] Corresponding author: sergi.claramunt@uab.cat

Abstract

Conductive Filaments (CF) in $Ni/HfO_2/Si$ resistive switching structures are analysed at the nanoscale by means of Conductive Atomic Force Microscopy (CAFM). Differences in the CF conductivity are measured depending on the resistive state of the device. Moreover, for both resistance states, non-homogeneous conduction across the CF area is observed, in agreement with a tree-shaped CF.

Keywords: Resistive switching, CAFM, metal-insulator-semiconductor (MIS).

1. Introduction

Resistive random access memories (RRAM) based on metal-insulator-metal (MIM) or metal-insulator-semiconductor (MIS) structures have emerged as promising candidates for substituting the present non-volatile memory technology [1]. In these structures, it is possible to electrically form and partially break a conductive filament (CF) through the insulator material, so that the dielectric resistance is changed. Then ON or OFF states are achieved, depending on the dielectric conductivity. This phenomenon is known as Resistive switching (RS). Moreover, the MIM (or MIS) structure can be easily fabricated using standard microfabrication techniques [2,3], opening the door to fully operational RRAM devices based on these structures [4,5]. In spite of that, before their integration at commercial level, the complex RS mechanism must be well understood [6]. Its analysis is complicated since the CF has a localized nature so that high spatial resolution techniques are required to evaluate their properties. For example, by combining Focused Ion Beam (FIB) and Transmission Electron Microscopy (TEM) it has been possible to observe the formation and dissolution of a CF in real time [7]. Another alternative is the use of Conductive Atomic Force Microscopy (CAFM) to switch the resistance of the dielectric material by using the conductive tip as the top electrode of the stack structure [8,9]. With this technique, it is possible to create and analyse the CFs locally with a relatively simple setup. However, since the switching characteristics are strongly dependent on the electrode material [10], the properties of the CF formed using the CAFM tip as a top electrode could differ from the ones generated in conventional MIS or MIM structures. To overcome this limitation, in this work, a CF is formed in $Ni/HfO_2/Si$ capacitors. Afterwards, the Ni electrode is removed and the CF properties analysed at the nanoscale with the CAFM tip. The objective is to give further insight into the RS mechanisms responsible for the formation and partial dissolution of CFs in these MIS structures.

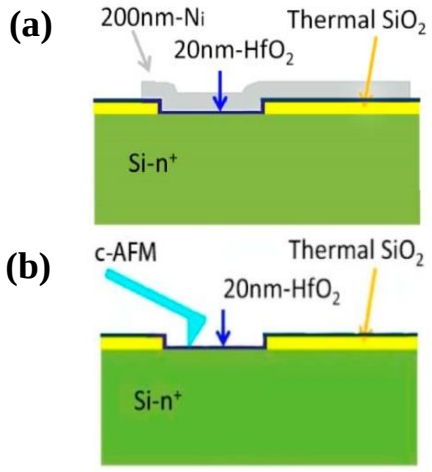

Fig.1. (a) Schematic cross-section of the studied $Ni/HfO_2/Si$ structures. (b) After Ni electrode removal, the whole active area of the device was scanned at constant voltage with the CAFM tip.

2. Materials and methods

A schematic cross-section of the studied Ni/HfO_2/Si capacitors [11] is shown in Fig. 1(a). The area of the devices is 5×5 μm^2. The structure and size was carefully chosen so that the whole active area of the device could be fully analysed by CAFM.

The methodology used consisted in first, creating the CF at device level with a HP-4155B semiconductor parameter analyser, using a current limit of 10^{-4} A. The voltage was applied to the Ni top electrode, while the Si substrate was grounded. To reach a stable state of the CF, five set and reset cycles were applied. Some samples were left at the high resistance state (HRS) while some others at the low resistance state (LRS). Fig. 2 shows the last I-V curves recorded after the set (left) and reset (right) processes in two different samples. In total, 10 samples were studied. After that, the Ni electrode of the MIS structures was etched off by means of (H_2O:HNO_3) (4:1) so as the HfO_2 surface was exposed and could be analysed with the tip of the CAFM (Fig 1b). A conductive Pt bulk tip with 20 nm nominal radius was used in order to study the device at the nanoscale. These tips are mechanically more stable than the metal-coated ones, permitting us to measure more maps without losing the topographical resolution and the conductivity during the experiments, a critical issue in measuring this type of systems. In any case, when small conductivity and/or resolution losses were observed, the tip was changed, so that the results are not affected by the tip properties. The whole active area was scanned at -4 V (injection from the substrate), so that the CF properties were not modified. For comparison, pristine samples and samples in which no current limit was stablished during electroforming have also been studied.

3. Results and discussion

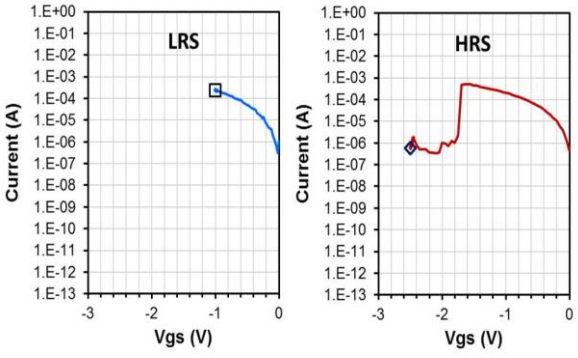

Fig 2. Last I-V curves of two of the studied samples that were left at the LR (left) and HR (right) states. The measurements have been obtained at device level with the semiconductor parameter analyser.

First, CAFM analysis of pristine samples was performed in order to study any possible effects of the etching of the top electrode on the HfO_2 layer (Fig. 3a). We found the oxide layer surface to be very uniform and no current was detected, meaning that the etching process had a negligible effect on the HfO_2 layer properties. Next, samples that underwent hard breakdown (i.e. without current limit) were studied (Fig 3b). In this case after Ni etching the topographical analysis showed an uncontrolled growth of a large structure covering the entire device surface, a consequence of the large energy dissipation caused by the irreversible dielectric breakdown of the oxide layer.

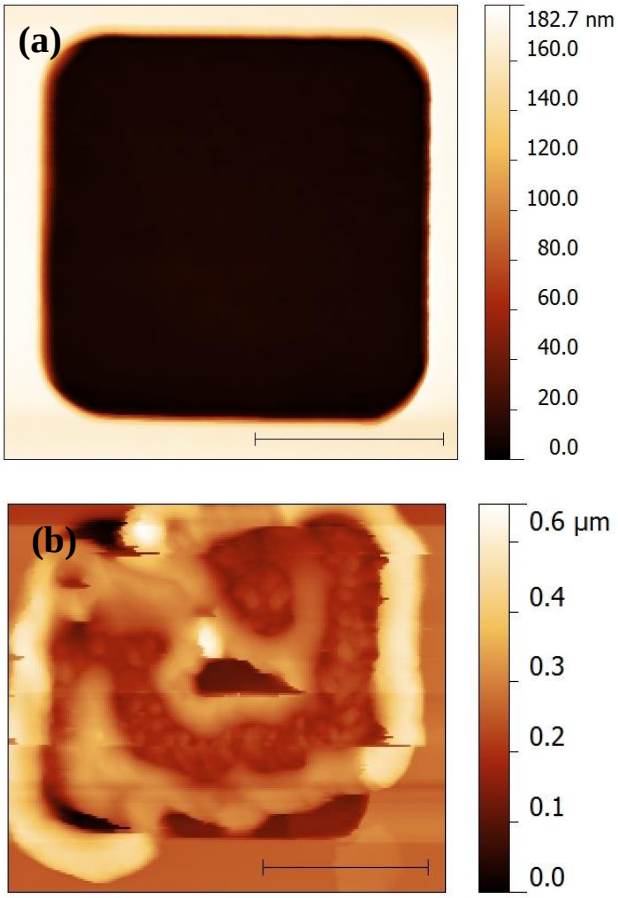

Fig. 3. (a) Topographical image of the pristine device after the etching of the Ni top electrode. A very flat surface is observed (b) Topographical image of a device after electroforming without current limit. A large morphological modification is measured. In both images the horizontal scale bar is 3µm.

The topography and current images measured on the rest of samples are significantly different. To show this point, Figure 4(a) and 4(b) present typical 2D topographical and current images, respectively, of

a device after the formation of the CF that was left at the HR state. Qualitatively similar results were obtained in the LRS samples. Interestingly, in the entire device surface only a hillock is detected, that corresponds to the sole conductive area found in the current image (Fig. 4b, Fig 4d). As can be seen in Figure 4c, which corresponds to the 3D topographical image of the hillock observed in Fig. 4a, the hillock has an irregular shape but presents well defined edges, demonstrating that the CF formation is local. In addition, the surface around the hillock is unaffected, and with the homogeneity of the pristine samples (see Fig 3(a)). This indicates that in our experimental conditions, one or several CFs are concentrated in the spot revealed by CAFM. This hillock is probably the result of the electrochemical and thermochemical reactions responsible for the CF formation and dissolution processes [12]. However, further analysis, which is out of the scope of this work, is needed to elucidate the physical origin of these morphological modifications.

After the analysis of several devices we observed that the position of the CF is random. Measurements show that the CF characteristics are qualitatively similar between devices, independently of the device state (i.e. LRS or HRS). We found that the spot areas are around 0.5 μm^2 with an estimated hillock height of around 100 nm. However, though a statistically representative analysis has not been carried out, the measurements seem to indicate that the LRS spots present smaller sizes (around 0.5X) than the HRS spots (Fig. 5).

Interestingly, as can be seen in Figure 5, the local conductive measurements of spots corresponding to LRS (a) and HRS (b) show that the current through the CF is not spatially homogeneous. Although in most of the spot area currents of pA are detected, there are small regions with currents in the range of nA. Moreover, in the LRS spots, the portion of the CF area with higher currents is larger than in the HRS, which would explain the larger LRS conductivity observed at device level (Figure 2). This inhomogeneous conduction is compatible with a tree-shaped CF [12]. As sketched in Figure 5 (c), some branches would span all along the dielectric thickness, connecting the two electrodes, whereas some others would end within the dielectric. Then, when scanning with the tip, larger currents would be measured in the first case (nA currents) whereas lower currents would be observed in the second case (pA currents). The number of electrode-connecting branches would be larger for the LRS case, in accordance with the observed size of the high-current area of the CF.

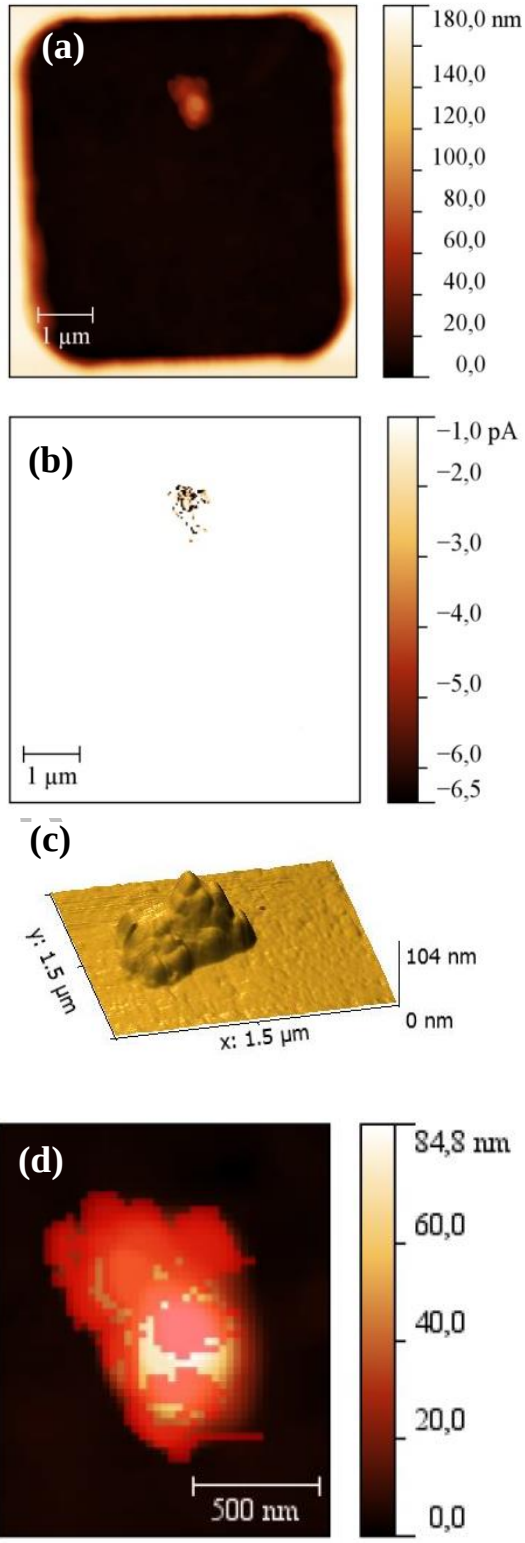

Fig. 4. (a) Topographical and (b) current images of a sample at the HRS state measured at -4 V. In both images, a unique spot is clearly visible in the device area. (c) Representation in 3D of the hillock. (d) Topographical image of the spot overlapping the current image (red colour), indicating that surface modifications and current increase are correlated.

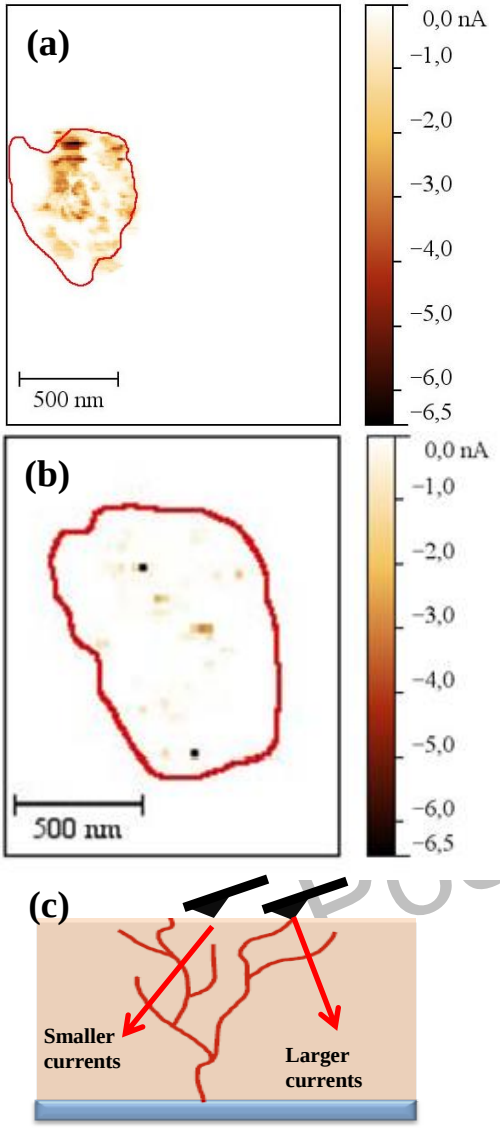

Fig. 5. Current images of representative spots corresponding to (a) LR and (b) HR states measured on different samples. The red line marks the edges of the regions where current is measured. (c) Schematic representation of the tree-shaped model of the CFs. The higher current measured with CAFM goes through the branches that end near the dielectric surface, whereas the others are responsible for the lower conductivity measured in the rest of the spot.

4. Conclusions

The CAFM characterization of CFs in Ni/HfO_2/Si RS structures is presented. We have shown that, independently of the device state (LRS or HRS) the CFs are formed in a unique spot that can be detected as a hillock in the topography image after the removal of the Ni electrode. Local electrical analysis of the HRS and LRS spots reveals a non-uniform conduction, with some regions in the spots with significantly higher conductivity. This behavior is in agreement with the tree-shaped model of CF formation.

Acknowledgments

This work has been partially supported by the Spanish MINECO and ERDF (TEC2013-45638-C3-1-R and TEC2011-27292-C02-02) and the Generalitat de Catalunya (2014SGR-384). Qian Wu acknowledges support from the Chinese Scholarship Council (No. 201408390030).

References

[1] R. Waser, M. Aono, Nat. Mater. 6 (2007) 833.
[2] Y.C. Yang, F. Pan, Q. Liu, M. Liu, F. Zeng, Nano Lett. 9 (2009) 1636.
[3] S. Song, B. Cho, T.W. Kim, Y. Ji, M. Jo, G. Wang, M. Choe, Y.H. Kahng, H. Hwang, T. Lee, Adv. Mater. 22 (2010) 5048.
[4] D.C. Sekar, B. Bateman, U. Raghuram, S. Bowyer, Y. Bai, M. Calarrudo, P. Swab, J. Wu, S. Nguyen, N. Mishra, R. Meyer, M. Kellam, B. Haukness, C. Chevallier, H. Wu, H. Qian, F. Kreupl, G. Bronner, IEEE IEDM 14, (2014) 657.
[5] K. Li, C. Ho, M. Lee, M. Chen, C. Hsu, J.M. Lu, C.H. Lin, C.C. Chen, B.W. Wu, Y.F. Hou, C.Y. Lin, Y.J. Chen, T.Y. Lai, M.Y. Li, I. Yang, C.S. Wu, F. Yang, IEEE Proc. Symp. VLSI Technol , (2014) 210.
[6] L. Zhao, Z. Jiang, H. Chen, J. Sohn, K. Okabe, B. Magyari-köpe, H.P. Wong, Y. Nishi, IEEE IEDM 14, (2014) 156.
[7] Q. Liu, J. Sun, H. Lv, S. Long, K. Yin, N. Wan, Y. Li, L. Sun, M. Liu, Adv. Mater. 24 (2012) 1774.
[8] M. Lanza, G. Bersuker, M. Porti, E. Miranda, M. Nafría, X. Aymerich, Appl. Phys. Lett. 101 (2012) 193502.
[9] S. Brivio, G. Tallarida, E. Cianci, S. Spiga, Nanotechnology 25 (2014) 385705.
[10] K.-L. Lin, T.-H. Hou, J. Shieh, J.-H. Lin, C.-T. Chou, Y.-J. Lee, J. Appl. Phys. 109 (2011) 084104.
[11] M.B. Gonzalez, J.M. Rafí, O. Beldarrain, M. Zabala, F. Campabadal, IEEE TDMR 14 (2014) 769.
[12] J. Lee, E.M. Bourim, W. Lee, J. Park, M. Jo, S. Jung, J. Shin, H. Hwang, Appl. Phys. Lett. 97 (2010) 172105.